





Methodology for Evaluating Equivalent Models for the Dynamic Analysis of Power Systems

Georgios A. Barzegkar-Ntovom  *Student Member, IEEE*, Eleftherios O. Kontis  *Member, IEEE*
Theofilos A. Papadopoulos  *Senior Member, IEEE*, and Panagiotis N. Papadopoulos  *Member, IEEE*

Abstract—The increasing penetration of distributed renewable energy sources drastically alters the dynamic characteristics of distribution networks (DNs). Therefore, several equivalent models have been recently proposed, to analyze more accurately the complex behavior of modern DNs. However, relatively simple models are still commonly used in practice for dynamic power system studies. In addition, dynamic equivalent models for DNs are sensitive to different operating conditions and there is lack of systematic understanding of their performance. Scope of this paper is to propose a methodology for identifying the applicability range in terms of accuracy and generalization capability of several conventional and newly developed equivalent models for the dynamic analysis of modern DNs. A set of metrics is used for the modelling accuracy assessment and a sensitivity analysis framework is introduced to fully quantify the generalization capabilities of DN equivalent models. Based on the above, guidelines and recommendations for the development of robust equivalent models for DN analysis are proposed.

Index Terms—Distribution networks, dynamic equivalencing, power system dynamics, sensitivity analysis.

I. INTRODUCTION

ACCURATE equivalencing of distribution networks (DNs) has a significant impact on the results of power system stability studies [1], [2]. Nevertheless, the majority of power system operators worldwide uses even nowadays simplistic approaches to integrate DNs in their stability studies. In particular, 70% of system operators worldwide still use static load models to represent DNs, while only about 30% of them use some form of dynamic equivalents [3]. Moreover, many system operators tend to adopt over-simplified approaches

concerning the modelling of distributed generation (DG), e.g., represent DGs as negative loads [3], [4].

Additionally, the advent of new non-conventional types of loads and mainly the increased penetration of converter-interfaced generators modify considerably the dynamic properties of DNs [5]. Thus, conventional equivalent models, developed a few decades ago and still used by system operators, progressively become obsolete failing to accurately simulate and analyze the complex behavior of modern DNs [6], [7].

Therefore, during the last years several equivalent models for DN analysis have been proposed in the literature [5], [8], [9], while power system operators have initiated a transition from the well-established static models to dynamic counterparts [10], [11]. Very recently, EPRI [12] has developed a dynamic equivalent model to represent converter-interfaced generators connected to DNs. The parameters of such models are known to be sensitive to changes in operating conditions. For example, [13] has highlighted the impact of system uncertainty on the parameters of a given dynamic equivalent model. However, this study is limited to one particular model and does not cover the array of available models which might already be adopted by system operators and planners. In this context, it is imperative to systematically identify to which extent the prevalent equivalent models can be used to analyze accurately the dynamic performance of modern active distribution networks (ADNs). This issue has not been sufficiently addressed in the literature. Most importantly, an assessment of the existing and newly proposed modelling approaches is required to evaluate the conditions, e.g. penetration levels of converter-interfaced generators and mixture of dynamic and static loads, under which each equivalent model can provide an acceptable accuracy.

The main motivation of this paper is to present a methodology to systematically evaluate the applicability of current dynamic equivalent models for changing network operating conditions. A large number of dynamic responses is generated, taking into account different network conditions and voltage disturbance levels; the simulated dynamic responses are used to derive parameters for various equivalent models following a measurement-based approach. The core of the methodology is to evaluate the derived models on the basis of two important aspects: accuracy and generalization capability (robustness), i.e., ability to represent network dynamics for a wide range of network conditions different to those originally developed [14], [15]. In this context, the paper provides the following contributions:

- A step-by-step procedure for equivalent model validation

G. A. Barzegkar-Ntovom and T. A. Papadopoulos are with the Power Systems Laboratory, Dept. of Electrical and Computer Engineering, Democritus University of Thrace, Xanthi, Greece, GR 67100, (e-mail: gbarzegk@ee.duth.gr; thpapad@ee.duth.gr).

E. O. Kontis is with the Power Systems Laboratory, School of Electrical and Computer Engineering, Aristotle University of Thessaloniki, Thessaloniki, Greece, GR 54124, and also with the Dept. of Electrical and Computer Engineering, University of Western Macedonia, Kozani, Greece, GR 50100, (e-mail: ekontis@auth.gr).

P. N. Papadopoulos is with the Institute for Energy and Environment, Dept. of Electronic and Electrical Engineering, University of Strathclyde, Glasgow, Scotland, G11QX, U.K. (e-mail: panagiotis.papadopoulos@strath.ac.uk).

The research work of G. A. Barzegkar-Ntovom was supported by the Hellenic Foundation for Research and Innovation (HFRI) under the HFRI PhD Fellowship grant (Fellowship Number: 1318).

The research work of E. O. Kontis, T. A. Papadopoulos and P. N. Papadopoulos was supported by the Hellenic Foundation for Research and Innovation (HFRI) under the “First Call for HFRI Research Projects to support Faculty members and Researchers and the procurement of high-cost research equipment grant” (Project Number: HFRI-FM17-229).

P. N. Papadopoulos was partly supported by the UKRI Future Leaders Fellowship MR/S034420/1. All results can be fully reproduced using the methods and data described in this paper and provided references.

TABLE I
EQUIVALENT MODEL STRUCTURES.

Equivalent Model	Type	Mathematical Representation	Number of Parameters
EXP f^1	Static	$y = y_0 \left(\frac{V}{V_0} \right)^{K_{yV}} [1 + K_{yf} \Delta f]$	EXP [16]: $N_T = 2$ EXP f [16]: $N_T = 4$
ZIP $f^{1,2}$	Static	$y = y_0 \left(p_1 \left(\frac{V}{V_0} \right)^2 + p_2 \left(\frac{V}{V_0} \right)^1 + p_3 \right) [1 + K_{yf} \Delta f]$	ZIP [16]: $N_T = 6$ ZIP f [16]: $N_T = 8$
EPRI f^1	Static	$P = P_0 \left(P_{a1} \left(\frac{V}{V_0} \right)^{K_{pv1}} [1 + K_{pf1} \Delta f] + (1 - P_{a1}) \left(\frac{V}{V_0} \right)^{K_{pv2}} \right)$ $Q = P_0 \left(Q_{a1} \left(\frac{V}{V_0} \right)^{K_{qv1}} [1 + K_{qf1} \Delta f] + \left(\frac{Q_0}{P_0} - Q_{a1} \right) \left(\frac{V}{V_0} \right)^{K_{qv2}} [1 + K_{qf2} \Delta f] \right)$	EPRI [17]: $N_T = 6$ EPRI f [17]: $N_T = 9$
PSS/E f^1	Static	$y = y_0 \left(a_1 \left(\frac{V}{V_0} \right)^{n_1} + a_2 \left(\frac{V}{V_0} \right)^{n_2} + a_3 \left(\frac{V}{V_0} \right)^{n_3} \right) [1 + a_4 \Delta f]$	PSS/E [18]: $N_T = 12$ PSS/E f [18]: $N_T = 14$
ZIP-EXP f^1	Static	$y = y_0 \left(\left(1 - (K_{yi} + K_{yc} + K_{y1} + K_{y2}) \right) \left(\frac{V}{V_0} \right)^2 + K_{yi} \left(\frac{V}{V_0} \right) + K_{yc} \right.$ $\left. + K_{y1} \left(\frac{V}{V_0} \right)^{nyv1} [1 + K_{yf1} \Delta f] + K_{y2} \left(\frac{V}{V_0} \right)^{nyv2} [1 + K_{yf2} \Delta f] \right)$	ZIP-EXP [19]: $N_T = 12$ ZIP-EXP f [19]: $N_T = 16$
ERM 3	Dynamic	$y = y_s - (y_s - y_t) \cdot e^{-\frac{t-t_0}{T_y}}$ $y_s = y_0 \left(\frac{V}{V_0} \right)^{N_s}, \quad y_t = y_0 \left(\frac{V}{V_0} \right)^{N_t}$	ERM [20]: $N_T = 6$ ERM-RPF [21], [22]: $N_T = 10$
Adaptive 3	Dynamic	$y = y_s - (y_s - y_t) \cdot e^{-\frac{t-t_0}{T_y/(V/V_0)^{N_t}}}$ $y_s = y_0 \left(\frac{V}{V_0} \right)^{N_s}, \quad y_t = y_0 \left(\frac{V}{V_0} \right)^{N_t}$	Adaptive [23]: $N_T = 6$ Adaptive-RPF: $N_T = 10$
TF-based	Dynamic	$y = f_1(V) + \mathcal{F}^{-1}[\mathcal{F}(f_2)G]$ $\hat{G}(s) = \sum_{m=1}^{m_o} \frac{c_m}{s-p_m} = \frac{\delta_\xi s^\xi + \delta_{\xi-1} s^{\xi-1} + \dots + \delta_0}{s^{m_o} + \gamma_{m_o-1} s^{m_o-1} + \dots + \gamma_0}$ $f_1(V) = y_0 (\lambda_1 (V/V_0) + \lambda_2), \quad \sum_{i=1}^2 \lambda_i = 1$ $f_2(V) = y_0 (\kappa_1 (V/V_0) + \kappa_2) - y_0 (\lambda_1 (V/V_0) + \lambda_2), \quad \sum_{i=1}^2 \kappa_i = 1$	Fourth-order [24]: $N_T = 26$
D-EXP 4	Composite	$y = a \cdot y_{exp} + b \cdot (a_{y1} \Delta y(k-1) + a_{y2} \Delta y(k-2) + c_{y0} \Delta V(k) + c_{y1} \Delta V(k-1) + c_{y2} \Delta V(k-2))$	D-EXP(1) [25]: $N_T = 10$ D-EXP(2) [25]: $N_T = 14$
D-ZIP 4	Composite	$y = a \cdot y_{zip} + b \cdot (a_{y1} \Delta y(k-1) + a_{y2} \Delta y(k-2) + c_{y0} \Delta V(k) + c_{y1} \Delta V(k-1) + c_{y2} \Delta V(k-2))$	D-ZIP(1) [25]: $N_T = 12$ D-ZIP(2) [25]: $N_T = 16$

¹For the frequency independent representation of the model, frequency dependent factors are neglected.

²For the ZIP model no constraints have been imposed for its parameters; this variant of ZIP is referred as ‘‘accurate ZIP model’’ [8].

³To extend the applicability of the model to simulate RPF phenomena [21], [22]: $y_s = y_0[\alpha_1(V/V_0) + \alpha_2]$, $y_t = y_0[\beta_1(V/V_0) + \beta_2]$.

⁴For the first order representation of the model, $a_{p2} = 0$ and $c_{p2} = 0$.

of both passive DNs and ADNs is introduced. The proposed methodology is intended to serve as general guidance for distribution system operators (DSOs) for selecting a valid approach to analyze DN dynamics.

- Considering the assessment of the model accuracy, a set of key performance indicators is adopted to properly quantify modelling errors. Regarding generalization capabilities, a new comprehensive sensitivity analysis procedure is introduced.
- The dynamic performance of existing most known and widely used equivalent models is evaluated. In the analysis, static, dynamic, composite and ADN-oriented models are considered.
- A critical overview and recommendations related to various aspects regarding dynamic equivalencing, e.g., model structure selection, is presented. This can offer valuable guidance to system operators and planners for the selection of appropriate models based on operating

conditions of the network (i.e. load mix and penetration of converter-interfaced generators).

II. POWER SYSTEM EQUIVALENT MODELS

In principle, static and dynamic models constitute the main two categories of equivalent models [8]. Static models describe the relationship of the real/reactive power at any time instant with the bus voltage and frequency; dynamic models express the real/reactive power as a function of voltage/frequency and time [8], [9].

To estimate model parameters, the measurement-based approach is predominantly used, since it is considered as the most reliable method [26]. In this work, time domain simulations are used as a substitute for real measurements [13], to evaluate the dynamic performance of DNs under a number of cases, e.g., load mixture, DG penetration level and voltage disturbance magnitude. Simulated responses are used to estimate parameters of several equivalent models; the examined

equivalent models are summarized in Table I. The model type, e.g., static, dynamic, etc., the corresponding mathematical formulation and the total number of real and reactive power model parameters, N_T , are also provided in Table I. Note that the mathematical formulations of the models that are valid for representing both real and reactive power dynamic responses are denoted by y . Nevertheless, some models use different mathematical expressions for representing real and reactive power responses; these formulations are explicitly denoted in Table I as P and Q , respectively.

As shown in Table I, five static models, which are usually available in existing commercial software packages, are considered, i.e., the exponential (EXP) [16], ZIP [16], EPRI [17], PSS/E [18], and ZIP-EXP [19]. In general, these models incorporate the dependency of active and reactive power on both voltage and frequency. However, in most of the existing works, only the voltage dependent term is taken into account, while the frequency dependent term is neglected [16]. In this paper two counterparts of the above-mentioned static equivalents are analyzed. In the first counterpart, only the voltage dependent term is considered. In the second type of counterparts, indicated by f , both voltage and frequency dependent terms are integrated to the model structure.

Five dynamic models are also studied. More specifically, the performance of the exponential recovery (ERM) [20] and the adaptive [23] models is investigated. Additionally, modified versions of them are examined, by adopting polynomial instead of the original exponential functions (for details, see footnote 3 of Table I). These variants can be used to simulate reverse power flow (RPF) phenomena which may occur in ADNs and are referred as ERM-RPF and Adaptive-RPF, respectively [21], [22]. Furthermore, a fourth-order transfer-function-based (TF-based) model, capable of capturing complex dynamics is employed [24].

In several studies, static and dynamic model structures have been combined constituting a more complex class of models, namely the composite. Typically, the static part of the composite model is represented in terms of ZIP or EXP form and the dynamic part by using either an induction motor (IM) model or expressions in differential form [25]. In this study, both ZIP and EXP static models augmented with first or second order difference equation based model structures are investigated, denoted as D-ZIP and D-EXP, respectively. In addition, the composite model represented by the ZIP model in parallel with a third-order IM model, i.e., ZIP-IM, is employed. Thus, five composite models are considered in total. The mathematical representation of the ZIP-IM ($N_T = 10$) is given in the Appendix.

During the last years, grey-box models have been also proposed in the literature for the analysis of ADNs. Nevertheless, the adoption of such models by DSOs is still limited [8]. The most known model, acknowledged also by the CIGRE WP C4.605 has been originally proposed in [6] and consists of a ZIP-IM model in parallel with a third-order synchronous generator and a back-to-back full converter model. This model, named ‘‘ADN model’’ hereafter, was further modified in [27], by applying a standard state-space decomposition procedure, to reduce the set of parameters to be identified; here, this

model is denoted as ‘‘modified ADN model’’. The state-space representations of the ADN model and its modified version are given in the Appendix; the number of parameters of these models is $N_T = 20$ and $N_T = 13$, respectively.

In this paper, $N_{eq} = 22$ equivalent models are considered. Specifically, five static models incorporating only the voltage dependent term, five static models incorporating both voltage and frequency dependent terms, five dynamic equivalents, five composite models and two ADN-oriented equivalents are examined. Note that for the rest of the paper, index j ($j = 1, \dots, N_{eq}$) denotes the discrete model structures.

III. PROPOSED METHODOLOGY

As discussed in the introduction, it is within the interest of this paper to develop a methodology to evaluate current modelling practices in terms of accuracy and robustness. The methodology comprises of four stages as illustrated in Fig. 1: a) data acquisition, b) derivation of equivalent models, by estimating proper model parameters, c) model accuracy assessment and d) generalization capability quantification. The proposed methodology is generalized in the sense that it can be readily applied by DSOs to analyze the dynamic performance of DN regardless the topology of the given DN, the penetration of DGs, the type of loads, etc. The rest of the section describes each stage in detail.

A. Data Acquisition

The proposed methodology relies on the simulation of a variety of dynamic responses. Given a network configura-

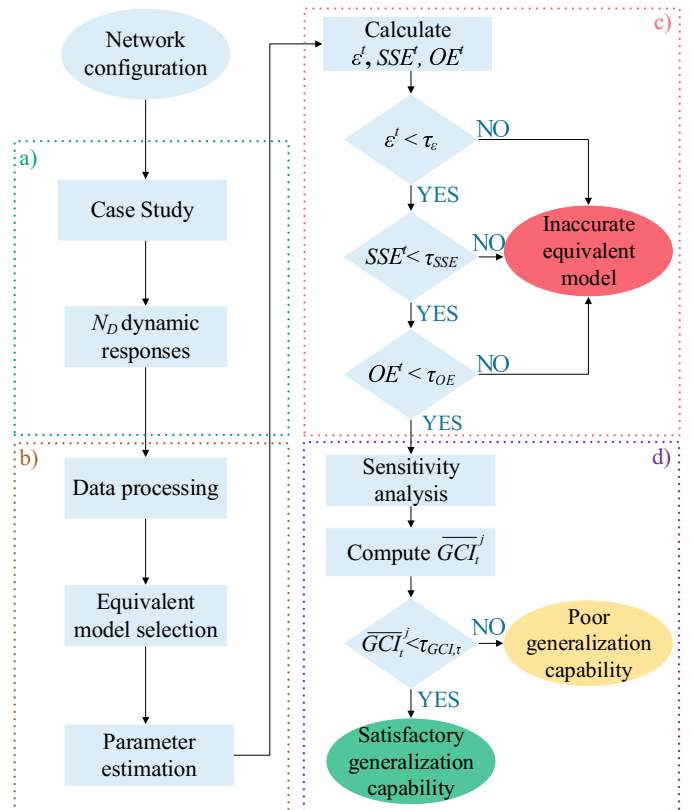


Fig. 1. Flowchart illustrating the proposed methodology.

tion, different case studies are examined; these case studies correspond to discrete load and generation mixes. For each case study, t , a set of N_D voltage disturbances are introduced, assuming discrete disturbance levels and operating conditions. Here, the operating conditions are defined by the pre-disturbance grid voltage level. The dynamic responses, resulted from the N_D disturbances, are used to derive equivalent models for the examined DN. For this purpose, all model structures summarized in Section II are used. Details about the examined case studies are provided in Section IV.

B. Derivation of Equivalent Models

Given a specific case study, the analysis starts by applying data processing to all simulation results, i.e., dynamic real and reactive power responses resulted by the N_D disturbances. Initially, the dynamic responses of real and reactive power are normalized to per unit (p.u.) values to minimize the deviation of the obtained model parameters [28]. In this work, normalization is performed using as base the values of the real and reactive power immediately after the disturbance. This approach is adopted to ensure that the overshoot error, analyzed in Section III-C, does not acquire infinite values, prohibiting the analysis of the results. Additionally, to facilitate parameter estimation and focus the investigation on dominant dynamics, redundant post-disturbance response samples are excluded from the analysis. In particular, for each dynamic response, n ($n = 1, \dots, N_D$), the optimal length of the analysis window, t_{ss} , is determined by applying the sliding window technique of [28]. The end of the window length is assumed, when the mean value of the latest acquired $|dP/dt|$ and $|dQ/dt|$ samples compared to the mean value of the newest ones is less than a predefined threshold, e.g., 10^{-4} . A common window length equal to the maximum of all resulting t_{ss} is determined for each case study.

The processed signals are used to identify model parameters of the examined equivalents, i.e., θ , using an identification method to fit input-output data; note that θ stands either for the real or reactive power parameter sets. Model parameters are estimated via the nonlinear least square optimization technique [8], aiming to minimize (1).

$$J = \sum_{k=1}^K (y_n[k] - \hat{y}_n[k])^2 \quad (1)$$

Here, K is the total number of response samples up to t_{ss} . $y_n[k]$ is the response of the actual system at the k -th sample of the n -th disturbance. Ideally, $y_n[k]$ is obtained via field measurements. In this work, instead of field measurements, responses from detailed RMS simulations are used. All simulations are performed using the DIGSILENT software [29]. The examined DN is presented in Section IV. \hat{y}_n is the real/reactive power estimated using one of the examined equivalents.

C. Model Accuracy Assessment

The performance of the examined equivalent models is statistically evaluated per case study using a set of metrics. In particular, for each case study, the accuracy of each model

is quantified in terms of the overall response by means of the relative error (ϵ^t), defined in (2).

$$\epsilon^t(\%) = \text{median} [\epsilon_1, \epsilon_2, \dots, \epsilon_n, \dots, \epsilon_{N_D}] \quad (2)$$

Here, ϵ_n is the relative error computed for each one of the available N_D responses ($n = 1, \dots, N_D$) as in (3) [30].

$$\epsilon_n(\%) = \frac{\left(\frac{1}{K} \sum_{k=1}^K (y_n[k] - \hat{y}_n[k])^2 \right)^{\frac{1}{2}}}{\left(\frac{1}{K} \sum_{k=1}^K y_n[k]^2 \right)^{\frac{1}{2}}} \cdot 100\% \quad (3)$$

Additionally, to quantify the error between the actual and the estimated post-disturbance steady-state power and the power overshoot, the steady-state relative error (SSE^t) and the overshoot relative error (OE^t), defined in (4) and (5), respectively, are used.

$$SSE^t(\%) = \text{median} [SSE_1, SSE_2, \dots, SSE_n, \dots, SSE_{N_D}] \quad (4)$$

$$OE^t(\%) = \text{median} [OE_1, OE_2, \dots, OE_n, \dots, OE_{N_D}] \quad (5)$$

SSE_n and OE_n are the steady-state and overshoot relative error calculated for the n -th dynamic response, as in (6) and (7), respectively.

$$SSE_n(\%) = \left| \frac{y_n^{ss} - \hat{y}_n^{ss}}{y_n^{ss}} \right| \cdot 100\% \quad (6)$$

$$OE_n(\%) = \left| \frac{y_n^+ - \hat{y}_n^+}{y_n^+} \right| \cdot 100\% \quad (7)$$

Here, y^{ss} is the new steady-state power, y^+ is the power immediately after the disturbance; \hat{y}^{ss} and \hat{y}^+ denote the corresponding estimates.

Indices ϵ^t , SSE^t and OE^t comprise the set of metrics used to assess the accuracy of the derived models per case study. As shown in (2), (4) and (5), ϵ^t , SSE^t and OE^t are defined as the median values of the corresponding indices computed using all N_D available dynamic responses contained at the t -th case. This way, the adopted set of metrics is used to statistically evaluate the distinct real and reactive power characteristics of each model structure per case study. Note that real and reactive power responses are separately evaluated by using (2) - (7).

The calculated ϵ^t , SSE^t and OE^t are checked against preset user-defined thresholds τ_ϵ , τ_{SSE} and τ_{OE} , respectively. Considering that at least one of the predefined thresholds is violated, the equivalent model is assumed inaccurate (marked with red color in Fig. 1) for the examined t -th case study. In this work, τ_ϵ , τ_{SSE} and τ_{OE} are considered equal to 5%. This way, the proposed method considers different and important aspects of the model performance and can provide useful and more detailed information to system operators and planners as well as flexibility to choose according to specific needs.

D. Generalization Capability Quantification

Let us assume a model structure j from Section II with set of real/reactive power parameters $\theta = [\theta_1, \theta_2, \dots, \theta_{N_{mp}^j}]$. N_{mp}^j denotes the number of the real/reactive power parameters; their sum is equal to N_T (see Table I). For each θ_i ($i = 1, 2, \dots, N_{mp}^j$) a set of estimates \mathbf{E}_i is obtained from the N_D disturbances.

In the literature, [13]–[15], it is common practice to evaluate the generalization capability of models by partitioning the available data into training and validation sets; the former is used to derive generic set of model parameters and the latter to validate their efficiency. Nevertheless, the development of a generic model that fits well to new, unseen disturbances generally depends on the method used to partition the data set, as well as the availability of plethora of dynamic responses [31]. In this work, to evaluate the robustness of the equivalent models per case study, the generalization capability index, \overline{GCI}_t^j , is introduced in (8), inspired by variance-based sensitivity analysis [32]. \overline{GCI}_t^j is a form of global sensitivity analysis and determines the standard deviation $\sigma^j(\mathbf{E}_i)$ of the i -th model parameter θ_i , against its representative value, $\mu^j(\mathbf{E}_i)$. In this way, the sensitivity of the model output with respect to the parameter variation can be quantified, even under a few known disturbances. Note that, \mathbf{E}_i is a $N_D \times 1$ vector containing the estimates of the i -th real/reactive power model parameter of the t -th case study.

$$\overline{GCI}_t^j = \frac{1}{N_{mp}^j} \cdot \sum_{i=1}^{N_{mp}^j} \frac{\sigma^j(\mathbf{E}_i)}{|\mu^j(\mathbf{E}_i)|} \quad (8)$$

It is evident from (8) that \overline{GCI}_t^j depends on N_{mp}^j . However, all model parameters are not of the same importance. Moreover, specific parameters of the ZIP-IM and ADN-oriented models are unobservable and unidentifiable from the signals [27], [33]. This implies that they have a minor influence on the model dynamics [33]. To ensure a fair comparison, \overline{GCI}_t^j is computed for each model on the basis of the most critical parameters (parameters that have significant influence on the model output). Recently, a variant of the least absolute shrinkage and selection operator technique has been proposed, to discard parameters with negligible impact [34]. In this work, an alternative approach to identify the critical model parameters, providing also an insight on the model dynamics, is proposed using a one-at-a-time sensitivity analysis as follows.

- The effect of parameter variation on the model output is investigated by using a dynamic reference response (for both the real and reactive power) per case study. The reference response is selected from the N_D responses and corresponds to the voltage disturbance with level equal to the median of all disturbances. For the reference response the model parameters, θ^{ref} , are identified.
- Subsequently, each i -th model estimate θ_i^{ref} ($\theta_i^{ref} \in \mathbf{E}_i$) is individually varied to specific limits, assuming the remaining parameters constant, and ϵ_n is computed. These limits are defined by the minimum and maximum parameter estimates of the remaining $N_D - 1$ responses.

Metric ϵ_n is used to quantify the mismatch between the reference response and the response obtained by applying the varied set of parameters. In this sense, in (3), $y_n[k]$ and $\hat{y}_n[k]$ correspond to the responses obtained with the reference and modified parameters, respectively. High ϵ_n values indicate a significant influence of the target model parameter. Therefore, a model parameter is considered as critical, if at least one of the two aforementioned parameter variations lead to ϵ_n higher than τ_ϵ ; this refers to both the real and reactive power.

Since for each equivalent the critical model parameters have been determined, (8) is used to quantify their robustness. Note that, a small \overline{GCI}_t^j reveals low dispersion and consequently a robust set of model parameters. This is an indication that in such a case, extracted model parameters will be able to be used for a wider range of operating conditions without significantly affecting the model performance. In this sense, an equivalent model is considered to present satisfactory generalization capabilities per case study if the corresponding \overline{GCI}_t^j is less than a pre-specified value, $\tau_{GCI,t}$. Instead of using a fixed value for each model, $\tau_{GCI,t}$ is determined per case study as the mean \overline{GCI}_t^j via (9); this way, the generalization capabilities performance of all $N_{eq} = 22$ equivalent models is taken into consideration upon calculating $\tau_{GCI,t}$.

$$\tau_{GCI,t} = \frac{1}{N_{eq}} \cdot \sum_{j=1}^{N_{eq}} \overline{GCI}_t^j \quad (9)$$

In Fig. 1, an accurate equivalent model with satisfactory generalization capabilities is highlighted with green color; lack of acceptable generalization capability is indicated with yellow color.

IV. TEST NETWORK AND CASE STUDIES

The efficiency of the derived models in dynamic equivalencing is evaluated by using as test system a modified version of the European MV benchmark DN proposed by CIGRE [35], illustrated in Fig. 2. Transformer and line parameters are

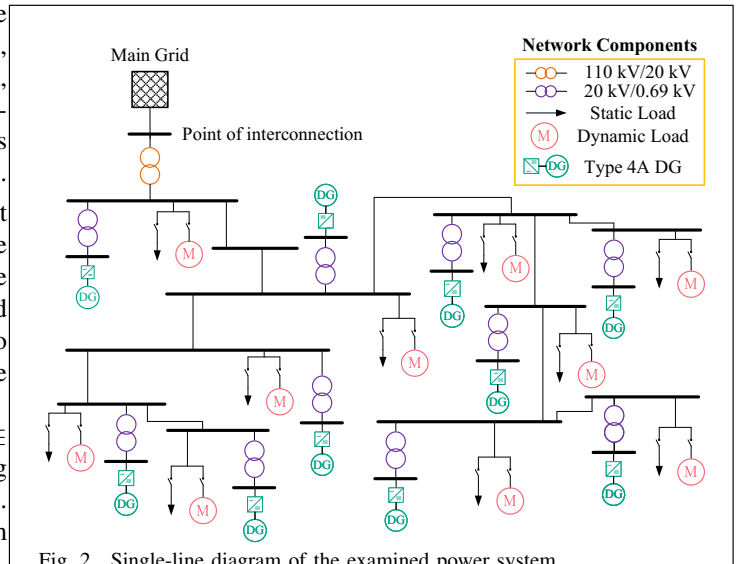


Fig. 2. Single-line diagram of the examined power system.

according to [35]. The dynamic performance of the examined system is analyzed by performing dynamic RMS simulations in DIgSILENT - PowerFactory [29].

The total system load is equal to 4590 kVA and it is uniformly distributed to system buses. Two main network operating scenarios are examined as follows:

- **Passive DN:** network end-users consist only of loads. The load composition is composed of the static and the dynamic part. Static loads (SLs) are modelled as constant impedance loads, while dynamic loads (DLs) using Type-7 IM model parameters [19]. $N_{DL} = 11$ case studies are examined by varying the DL participation in the total system load. Specifically, the dynamic part varies from 0% to 100% with a 10% step, whereas the static part changes accordingly to reach the 100% load mixture.
- **ADN:** the examined system is further modified by evenly adding DG units to all system buses. DGs are modelled using the type 4a model [36]. A type 4 model characterizes converter-interfaced generation (wind generators, PV units, etc.) [4]; note that although this model embeds voltage support functionalities, within the examined range of voltage disturbances, they are not activated. The rated power of the load is assumed constant; the proportion of SL and DL is 40% and 60%, respectively, which is typical for developed countries [37]. $N_{DG} = 10$ case studies are considered, assuming DG penetration levels varying from 10% to 100% with a 10% step in terms of the total system load power.

Since the network dynamic performance is also significantly affected by the pre-disturbance voltage level at the point of interconnection, three different operating conditions (discrete voltage levels) within the range $0.95 \div 1.05$ p.u. are considered for the different case studies. In total $N_D = 20$ step-down and step-up disturbances, varying from -0.1 p.u. up to 0.1 p.u., are caused at the secondary side of the 110kV/20kV transformer by tap changing. Hence, $N_{PAS} = N_{DL} \cdot N_D = 220$ and $N_{ADN} = N_{DG} \cdot N_D = 200$ responses are generated for the passive DN and the ADN scenario, respectively.

V. PERFORMANCE ANALYSIS OF EXAMINED MODELS

In this Section, the accuracy and the generalization capability of the examined models are evaluated via simulated responses using the methodology proposed in Section III.

A. Demonstration Example

Initially, estimated responses derived using the examined equivalent models are compared to the original system responses obtained using the detailed power system model implemented in DIgSILENT. In Figs. 3 and 4, indicative instances of real and reactive power modelling are depicted, corresponding to case studies characterized by 100% DL participation and 100% DG penetration, respectively. The performance of the EXP, ZIP-EXPF, ERM, D-ZIP(1) and ADN models is examined; in these figures the error metric results are also summarized. Indicatively, one model from each category (frequency-independent and -dependent static, dynamic, composite and ADN-oriented) is arbitrarily selected

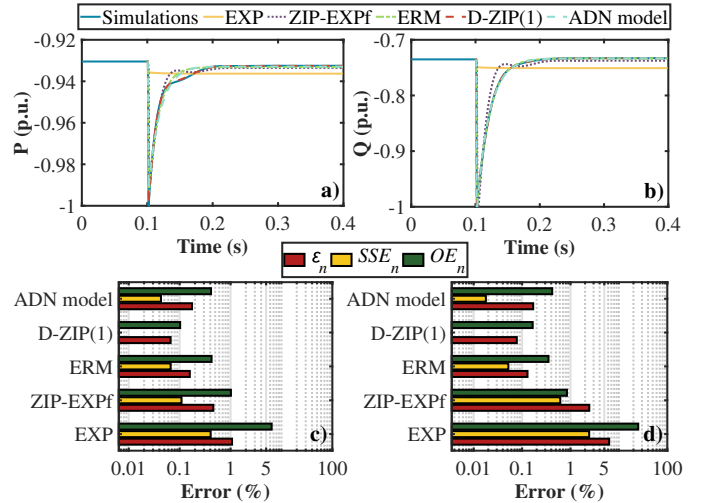


Fig. 3. a) Real and b) reactive power modelling of a random instance of the N_{PAS} responses, assuming 100% DL participation; corresponding c) real and d) reactive power error metric results.

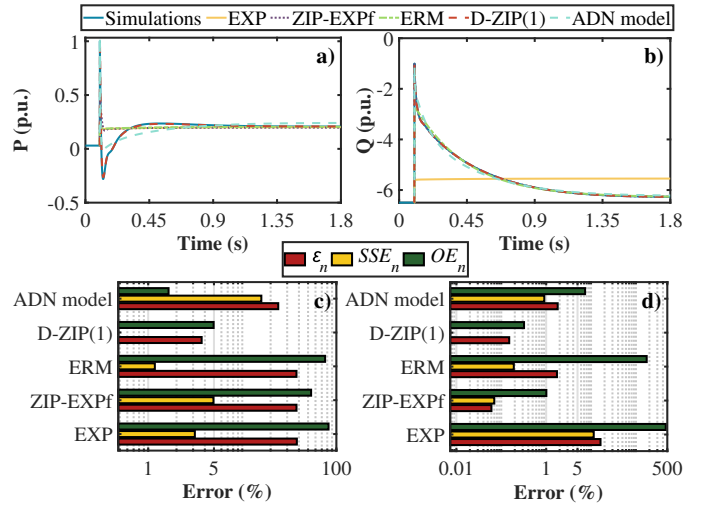


Fig. 4. a) Real and b) reactive power modelling of a random instance of the N_{ADN} responses, assuming 100% DG penetration; corresponding c) real and d) reactive power error metric results.

for demonstration purposes. Note that in Figs. 3a and 3b, as well as in Figs. 4a and 4b, a minus sign denotes that the examined DN consumes power; a plus sign indicates generation of power which flows towards the upstream grid.

From Fig. 3a and 3b, it is evident that the ZIP-EXPF, ERM, D-ZIP(1) and ADN model represent with high accuracy the distinct real and reactive power characteristics of the examined system; this is also verified by the corresponding error metric results presented in Figs. 3c and 3d. On the contrary, the EXP model cannot capture the power overshoot; indeed, significant (higher than τ_{OE}) real and reactive power OE_n is computed. Considering the results of Fig. 4, it is clear that the EXP model fails to represent the dynamic behavior of the ADN, estimating accurately only the new steady-state real power. The ZIP-EXPF, ERM and ADN model cannot accurately simulate the complex real power system dynamics; ERM and ADN model present also significant reactive power OE_n . On the other hand, D-ZIP(1) satisfactorily simulates the real and reactive power responses, capturing the overshoot, the oscillations and the new steady-state. From Fig. 4a, it is also

shown that the ERM cannot simulate the RPF after the voltage disturbance. In such cases, to accurately replicate real/reactive power overshoots, the ERM modified version, i.e., ERM-RPF, shall be adopted.

B. Statistical Analysis of Performance Metrics

The modelling accuracy of the derived equivalents is thoroughly assessed by analyzing the error metric results. In Figs. 5 and 6, the real and reactive power ϵ^t and OE^t for the passive DN analysis (N_{DL} case studies) are summarized, respectively, by means of heat maps. Overall, ϵ^t and OE^t increase with the DL participation in the load mix. As shown, concerning the real power modelling, the examined equivalents provide in all cases ϵ^t errors lower than τ_ϵ . Additionally, reactive power results reveal that frequency-independent static models present significant ϵ^t (higher than τ_ϵ), when the dynamic part in the total load mixture is higher than 20%.

By assessing the OE^t results of Fig. 6, it can be realized that the power overshoot cannot be accurately captured by frequency-independent static models; indeed, significant real and reactive power OE^t (higher than τ_{OE}) are observed in almost all cases. In general, frequency-independent static models present increased ϵ^t and OE^t for reactive power (compared to real power), indicating that reactive power modelling is more challenging. It is worth noting that for all N_{DL} case studies, all examined equivalents present SSE^t less than τ_{SSE} , regardless of the DL participation level; hence, SSE^t heat maps are omitted for brevity. This remark actually denotes that all examined equivalent models can be used for steady-state analysis, e.g., power flow calculation.

The resulting ϵ^t and OE^t for the ADN analysis (N_{DG} case studies) are presented in Figs. 7 and 8, respectively. In general, higher error metric values are observed for the ADN analysis compared to passive DN analysis. These higher errors practically demonstrate that DG penetration has a significant impact on DN dynamics. Results of Fig. 7a reveal that the examined models preserve high accuracy for real power simulation in cases characterized by DG penetration up to 80%. High ϵ^t is observed for the frequency-independent static models and the EXPf, assuming 90% DG penetration; also, all examined equivalents (except first- and second-order D-EXP and D-ZIP)

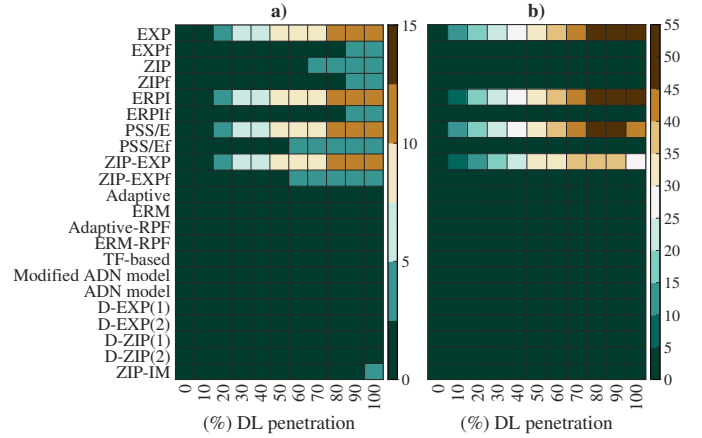


Fig. 6. OE^t for the a) real and the b) reactive power modelling of passive DNs as a function of DL participation.

exhibit significant ϵ^t , considering 100% DG penetration level. Indeed, in 100% DG penetration level, significant real power oscillations are observed that cannot be simulated accurately by all other models. In fact, only the TF-based model can provide satisfactory estimates by using higher order transfer functions. The reactive power ϵ^t , illustrated in Fig. 7b, reveals that most examined equivalents generally provide ϵ^t errors lower than τ_ϵ . In particular, high ϵ^t is only observed for the EXP model, indicating that it cannot capture the reactive power responses of the ADN; this is a significant remark, since about 72% of power system operators worldwide still use the EXP model to represent DN in stability studies [3]. In some cases, high ϵ^t is also observed for the EPRI, PSS/E, as well as for the EXPf equivalent models.

Based on the results of Fig. 8, it can be deduced that frequency-independent static models generally present significant real and reactive power OE^t . Also, from Fig. 8a, it is evident that real power OE^t increases with the DG penetration level. In low-to-moderate DG penetration conditions (up to 40%), frequency-dependent static models and ZIP-IM accurately capture the real power overshoot. The ERM, Adaptive and their modified versions present considerable real power OE^t at DG penetration levels of 90% or greater; this is also the case for the ADN-oriented equivalents. On the other hand, in all N_{DG} case studies, real and reactive

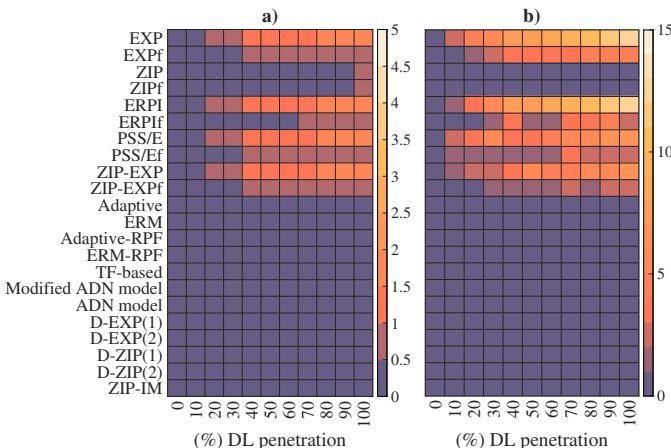


Fig. 5. ϵ^t for the a) real and the b) reactive power modelling of passive DNs as a function of DL participation.

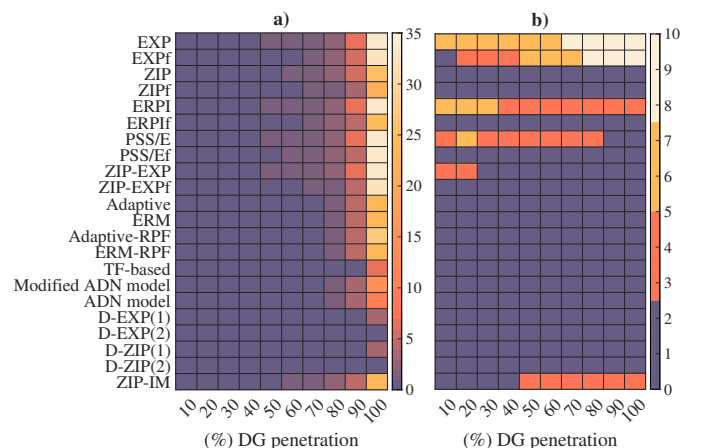


Fig. 7. ϵ^t of the a) real and the b) reactive power modelling of ADNs as a function of DG penetration.

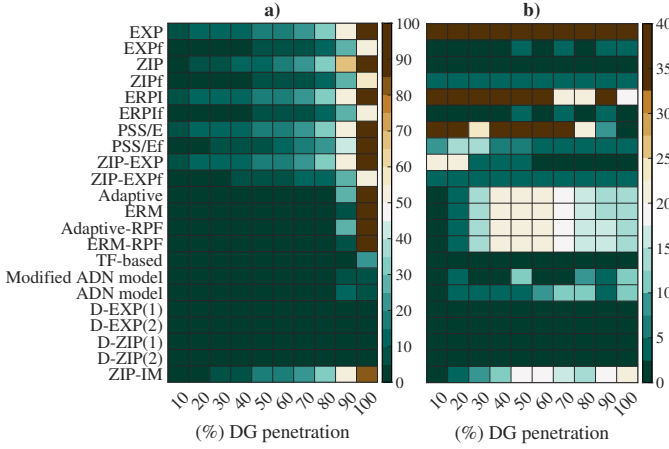


Fig. 8. OE^t of the a) real and the b) reactive power modelling of ADNs as a function of DG penetration.

power OE^t is less than τ_{OE} for the difference equation based models and the fourth-order TF-based model. By assessing the results of Fig. 8b, it is clear that the ERM, Adaptive and their modified versions present significant OE^t at DG penetration levels of 30% or greater; this also applies for the ZIP-IM model. Results of the ADN-oriented models reveal that the reactive power overshoot is accurately captured for DG penetration levels up to 50%. Frequency-dependent static models provide generally better estimates compared to their frequency-independent counterparts.

It is worth noting that both counterparts of static models (excluding ZIP and ZIPf) present real power SSE^t higher than τ_{SSE} at DG penetration level of 100%. Also, reactive power SSE^t higher than τ_{SSE} was observed for the EXP and EXPf models, considering more than 50% DG penetration. Thus, it can be concluded that the new steady-state power cannot be accurately captured by static models under high DG penetration levels.

C. Generalization Capability Assessment

The robustness of each model structure, j , is assessed per case study by comparing the \overline{GCI}_t^j index, calculated using (8), with the resulting $\tau_{GCI,t}$ from (9). Recall that lower \overline{GCI}_t^j indicates increased model robustness.

In Fig. 9, the mean \overline{GCI}_t^j for the passive DN and ADN cases are presented. Specifically, for each equivalent model the arithmetic mean of the \overline{GCI}_t^j values, as derived from the available N_{DL} and N_{DG} case studies is computed and summarized as bars in Figs. 9a and 9b, respectively. Note that the mean real and reactive power $\tau_{GCI,t}$, i.e., $\overline{\tau_{GCI}}$, is also depicted in the same figures (dashed lines); real/reactive power $\overline{\tau_{GCI}}$ is determined as the mean $\tau_{GCI,t}$ computed from the corresponding case studies of the passive DN and ADN.

From the obtained results it can be generally concluded that equivalent models with increased number of parameters present high \overline{GCI}_t^j values compared to simpler equivalent models. In particular, the Adaptive, ERM and their modified versions as well as the EXP model, result in the lowest \overline{GCI}_t^j values. On the contrary, high \overline{GCI}_t^j values are observed for the ZIP, ZIPf, EPRI, ZIP-EXPf, D-EXP(2), D-ZIP(1) and the modified ADN equivalents.

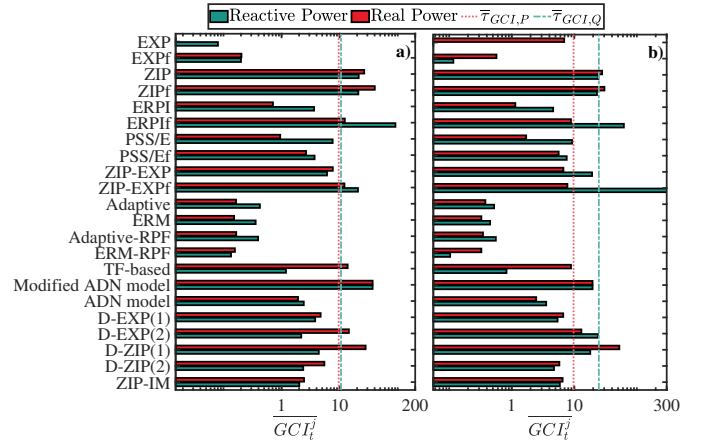


Fig. 9. Resulting mean real and reactive power \overline{GCI}_t^j for the a) passive DN and b) ADN analysis. Results are illustrated using a logarithmic scale.

D. Computational Efficiency

Next, the examined equivalent models are evaluated in terms of computational burden by quantifying the execution time required to estimate model parameters. The execution time for the modelling of the N_{PAS} and N_{ADN} responses is summarized in Fig. 10 by means of violin plots; violin plots are used to visualise the distribution and probability density of the data in detail [38]. Calculations were performed using an i7-8550U, 1.8 GHz, RAM 8 GB personal computer. The analysis reveals that the computational burden highly depends on the number of model parameters, N_T , that must be determined, as well as on the complexity of the model structure. Among the examined equivalents, static models exhibit the lowest average computational burden, whereas the ZIP-IM and ADN-oriented equivalents the highest. Nevertheless, since parameter estimation is generally performed offline, the presented computational burden is considered acceptable for all models, ranging from tens of milliseconds to some hundreds of seconds.

VI. OVERALL ASSESSMENT OF THE EXAMINED EQUIVALENTS AND MODELLING RECOMMENDATIONS

Table II investigates the performance of the examined equivalent models in terms of accuracy and generalization

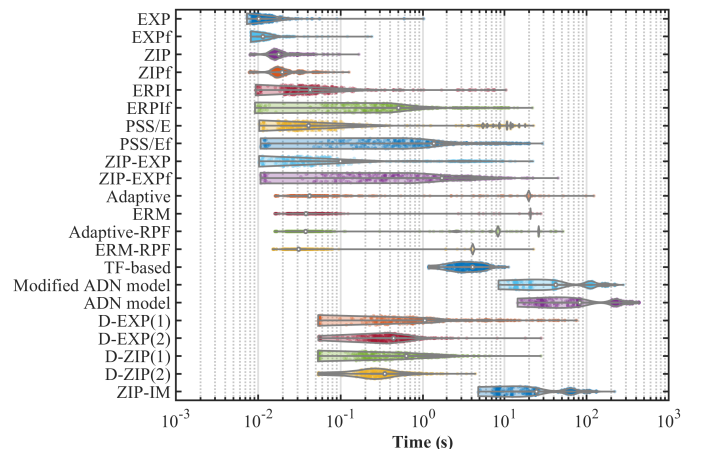


Fig. 10. Violin plots of the required execution time for real and reactive power modelling. Results are illustrated using a logarithmic scale.

TABLE II
PERFORMANCE SUMMARY OF THE EXAMINED EQUIVALENT MODELS FOR THE DYNAMIC ANALYSIS OF PASSIVE DNS AND ADNS.

Model structure	DL participation (%)											*DG penetration level (%)									
	0	10	20	30	40	50	60	70	80	90	100	10	20	30	40	50	60	70	80	90	100
EXP	Green	Red	Red	Red	Red	Red	Red	Red	Red	Red	Red	Red	Red	Red	Red	Red	Red	Red	Red	Red	Red
EXP _f	Green	Green	Green	Green	Green	Green	Green	Green	Green	Green	Green	Green	Green	Green	Green	Green	Green	Green	Green	Green	Green
ZIP	Yellow	Yellow	Yellow	Yellow	Yellow	Yellow	Yellow	Yellow	Yellow	Yellow	Yellow	Yellow	Yellow	Yellow	Yellow	Yellow	Yellow	Yellow	Yellow	Yellow	Yellow
ZIP _f	Yellow	Yellow	Yellow	Yellow	Yellow	Yellow	Yellow	Yellow	Yellow	Yellow	Yellow	Yellow	Yellow	Yellow	Yellow	Yellow	Yellow	Yellow	Yellow	Yellow	Yellow
EPRI	Green	Red	Red	Red	Red	Red	Red	Red	Red	Red	Red	Red	Red	Red	Red	Red	Red	Red	Red	Red	Red
EPRI _f	Green	Green	Green	Green	Green	Green	Green	Green	Green	Green	Green	Green	Green	Green	Green	Green	Green	Green	Green	Green	Green
PSS/E	Green	Red	Red	Red	Red	Red	Red	Red	Red	Red	Red	Red	Red	Red	Red	Red	Red	Red	Red	Red	Red
PSS/E _f	Green	Green	Green	Green	Green	Green	Green	Green	Green	Green	Green	Green	Green	Green	Green	Green	Green	Green	Green	Green	Green
ZIP-EXP	Yellow	Red	Red	Red	Red	Red	Red	Red	Red	Red	Red	Red	Red	Red	Red	Red	Red	Red	Red	Red	Red
ZIP-EXP _f	Green	Yellow	Yellow	Yellow	Yellow	Yellow	Yellow	Yellow	Yellow	Yellow	Yellow	Yellow	Yellow	Yellow	Yellow	Yellow	Yellow	Yellow	Yellow	Yellow	Yellow
Adaptive	Green	Green	Green	Green	Green	Green	Green	Green	Green	Green	Green	Green	Green	Green	Green	Green	Green	Green	Green	Green	Green
ERM	Green	Green	Green	Green	Green	Green	Green	Green	Green	Green	Green	Green	Green	Green	Green	Green	Green	Green	Green	Green	Green
Adaptive-RPF	Green	Green	Green	Green	Green	Green	Green	Green	Green	Green	Green	Green	Green	Green	Green	Green	Green	Green	Green	Green	Green
ERM-RPF	Green	Green	Green	Green	Green	Green	Green	Green	Green	Green	Green	Green	Green	Green	Green	Green	Green	Green	Green	Green	Green
TF-based	Yellow	Yellow	Yellow	Yellow	Yellow	Yellow	Yellow	Yellow	Yellow	Yellow	Yellow	Yellow	Yellow	Yellow	Yellow	Yellow	Yellow	Yellow	Yellow	Yellow	Yellow
Modified ADN model	Yellow	Green	Green	Green	Green	Green	Green	Green	Green	Green	Green	Green	Green	Green	Green	Green	Green	Green	Green	Green	Green
ADN model	Green	Green	Green	Green	Green	Green	Green	Green	Green	Green	Green	Green	Green	Green	Green	Green	Green	Green	Green	Green	Green
D-EXP(1)	Green	Yellow	Yellow	Yellow	Yellow	Yellow	Yellow	Yellow	Yellow	Yellow	Yellow	Yellow	Yellow	Yellow	Yellow	Yellow	Yellow	Yellow	Yellow	Yellow	Yellow
D-EXP(2)	Green	Yellow	Yellow	Yellow	Yellow	Yellow	Yellow	Yellow	Yellow	Yellow	Yellow	Yellow	Yellow	Yellow	Yellow	Yellow	Yellow	Yellow	Yellow	Yellow	Yellow
D-ZIP(1)	Green	Green	Green	Green	Green	Green	Green	Green	Green	Green	Green	Green	Green	Green	Green	Green	Green	Green	Green	Green	Green
D-ZIP(2)	Green	Green	Green	Green	Green	Green	Green	Green	Green	Green	Green	Green	Green	Green	Green	Green	Green	Green	Green	Green	Green
ZIP-IM	Yellow	Green	Green	Green	Green	Green	Green	Green	Green	Green	Green	Green	Green	Green	Green	Green	Green	Green	Green	Green	Green

■ Accurate equivalent model presenting satisfactory generalization capability.
■ Accurate equivalent model exhibiting relatively low generalization capability.
■ Inaccurate equivalent model.

* The proportion of SL and DL is 40% and 60%, respectively.

capability. Results are presented as a function of the DL participation and the DG penetration for the passive DN and ADN analysis, respectively. Table II is formed taking into consideration the resulting real and reactive power ϵ^t , SSE^t and OE^t , as well as the \overline{GCI}_t^j per case study; results are highlighted with distinct colors. In particular, an equivalent model that provides simultaneously ϵ^t , SSE^t and OE^t , lower than 5% and also presents high generalization capabilities, i.e., $\overline{GCI}_t^j < \tau_{GCI,t}$ is indicated with green color. An equivalent model that satisfies modelling error criteria but presents $\overline{GCI}_t^j > \tau_{GCI,t}$ is indicated with yellow color. On the other hand, a red color implies that the examined equivalent is inaccurate, i.e., one of ϵ^t , SSE^t or OE^t is higher than 5%.

Hereafter, key research findings are summarized and practical guidelines for the dynamic analysis of DNs are provided: **Passive DNs:** Based on the results of Table II, three groups of equivalents can be identified. The first group includes the frequency-independent static models (apart from the ZIP model). The models of this group cannot be used for the dynamic equivalencing of DNs, since they provide accurate results only when the DL participation in the load mix is less than 10%. In all other cases, the above-mentioned models do not provide acceptable accuracy, resulting in modelling errors higher than 5%. The second group consists of ZIP, ZIP_f, EPRI_f, ZIP-EXP_f, TF-based model, D-EXP(2) and D-ZIP(1) models. Models belonging to this group can provide accurate estimates under all examined DL participation scenarios, capturing precisely the overshoot, the new steady-state and the overall dynamic response of both real and reactive power. However, these models present in many cases limited generalization capabilities. In fact, to generalize the parameters

of these models, sophisticated techniques are required, e.g., [15]. The third group of equivalents includes the EXP_f model, the PSS/E_f, the Adaptive and the ERM as well as their modified versions, the D-EXP(1) and D-ZIP(2) models, and finally the ZIP-IM model. Models that belong in this third group present high accuracy and simultaneously high generalization capabilities. Therefore, they can be used for the derivation of generic equivalent models for passive DN analysis.

ADNs: Accordingly, for the ADN analysis, equivalent models can be classified into four groups. The frequency-independent static models and PSS/E_f comprise the first group; these models should be avoided for the dynamic equivalencing of ADNs, since they do not provide acceptable accuracy. The second group includes the ZIP-IM and the first-order dynamic models; these models provide accurate estimates up to 20% DG penetration levels and simultaneously present low \overline{GCI}_t^j , inferring satisfactory generalization capabilities. This is a significant conclusion since the aforementioned equivalents constitute some of the most well-studied model structures for DN analysis. Note that despite the fact that the ERM-RPF and Adaptive-RPF models are capable of capturing possible RPF phenomena, almost identical error metric results to those of ERM and Adaptive are obtained; thus, the applicability range does not differ between the variants. The third group is composed of the frequency-dependent static models and the ADN-oriented equivalents. These models can be effectively applied to simulate accurately power responses of ADNs under moderate DG penetration conditions; however, increased model robustness is only observed for the ADN model and the EXP_f. It should be mentioned that the introduced step voltage disturbances lead to small instantaneous frequency

changes; thus, static models which consider frequency dependence may also capture the power overshoot immediately after the voltage disturbance. Note also that although the ADN-oriented equivalents were originally developed for the dynamic analysis of ADNs, here, they are considered inaccurate for high DG penetration conditions due to the significant reactive power OE^t , i.e., higher than τ_{OE} (see Fig. 8). The fourth group includes the difference equation based models and the fourth-order TF-based model; as it is shown, these models accurately replicate the complex dynamic responses of the ADN regardless of the DG participation. Nevertheless, limited generalization capability is presented for the D-EXP(2), D-ZIP(1) in all cases, as well as for the fourth-order TF-based model for very high DG penetration conditions. It is worth noting that D-ZIP and D-EXP are practically numerical models that represent the time-varying response of the DN. Since past values of voltage and power are considered within the model structures (see Table I), difference equation based models present superior modelling accuracy.

Note that all the above-mentioned remarks have been drawn assuming that modelling errors up to 5% are considered acceptable; the use of different thresholds would slightly differentiate the concluding remarks. Although the outcomes of this study may present differences to case studies for different DN configurations, the proposed approach would be equally applicable; thus, the proposed methodology is considered as generalized in the sense that it can be applied to any DN.

VII. DISCUSSION AND CONCLUSION

The main aim of this paper is to propose a systematic methodology to assess prevalent equivalent models in terms of modelling accuracy and generalization capability in order to inform about the appropriateness of their applicability for various DN operating conditions, i.e., different load mix and amount of connected converter interfaced generation.

The effectiveness of 22 equivalent models, including all categories, i.e., frequency-independent and -dependent static, dynamic, composite and ADN-oriented, has been investigated on a typical DN. Two network operating scenarios, i.e. passive DN and ADN, are assumed and different case studies are considered, to account for distinct load compositions and DG penetration levels. To evaluate the performance of the developed models in replicating the distinct real/reactive power characteristics, a set of indices from the literature is adopted and modified in a probabilistic manner. Additionally, a robustness assessment procedure is formulated, to quantify the generalization capability of the derived models.

Several factors are considered by power system operators when selecting the most appropriate model structure, e.g., ease of integration into commercial power system analysis software, complexity, necessity for physical meaning of model parameters, etc. In summary, the performed numerical studies indicate that all examined DN equivalent models exhibit similar behavior regarding the accurate estimation of the new steady-state power; differences are mainly observed regarding their capability to accurately capture the overall response, as well as the power overshoot. Therefore, the majority of them can be used for steady-state analysis, e.g., load flow

analysis. In such cases, relatively simple static models, e.g., EXP or ZIP, are suggested; these models have a limited number of parameters, and thus, can be updated on a regular basis by system operators to ensure accurate simulation results. Additionally, investigations have revealed that the inclusion of both IMs and DG units has a significant impact on the complexity of DN dynamics. In general, results indicated that several robust equivalent models exist for representing accurately the dynamic performance of passive DNs. Nevertheless, first-order dynamic equivalents should be generally preferred, e.g., the modified ERM/Adaptive versions, since they are computationally efficient, presenting high accuracy, as well as satisfactory generalization capabilities. To efficiently analyze the more demanding in terms of complexity and modelling requirements dynamic performance of ADNs, especially under high DG penetration conditions, advanced models should be adopted, e.g., high-order TF-based, difference equation based or ADN-oriented models. Since time-series models, such as the examined difference equation based models, cannot be easily integrated to power system simulation software and lack of physical meaning for their parameters, high-order TF-based or ADN-oriented models are suggested.

Generally, a model structure may fail to consistently provide optimal results for different data sets. Motivated by this challenge, this paper proposes a generalized methodology that can be employed by system operators and planners to identify robust equivalent models and parameter sets concerning their specific network configuration, while keeping a high accuracy; note that the proposed methodology was also applied to a different network configuration verifying its generic nature. Nevertheless, in cases where the adoption of the methodology is not possible, the findings of the conducted analysis can serve as a basis for selecting a valid approach with known compromises and details around them (e.g. choose low performance in terms of overshoot modelling but good performance in terms of steady-state behaviour) for the analysis of DNs.

APPENDIX

The ADN-model proposed in [6], [7] consists of a ZIP-IM model in parallel with a third-order synchronous generator model and a back-to-back full converter model. The ZIP-IM model is described by (10)-(11).

$$\frac{dE'_m}{dt} = \frac{1}{T'_{dm}} \left(-\frac{X_m}{X'_m} E'_m + \left(\frac{X_m - X'_m}{X'_m} \right) V \cos \delta_m \right) \quad (10a)$$

$$\frac{d\delta_m}{dt} = \omega_m - \omega_s - \left(\frac{X_m - X'_m}{X'_m} \right) \frac{V}{T'_{dm} E'_m} \sin \delta_m \quad (10b)$$

$$\frac{d\omega_m}{dt} = -\frac{1}{H_m} \left(\frac{E'_m V}{X'_m} \sin \delta_m + T_m \right) \quad (10c)$$

$$P_L = P_{ZIP0} \left[P_Z \left(\frac{V}{V_o} \right)^2 + P_I \left(\frac{V}{V_o} \right)^1 + P_P \right] - \left(\frac{V}{X'_m} E'_m \sin \delta_m \right) \quad (11a)$$

$$Q_L = Q_{ZIP0} \left[Q_Z \left(\frac{V}{V_o} \right)^2 + Q_I \left(\frac{V}{V_o} \right)^1 + Q_Q \right] + \left(\frac{V^2}{X'_m} - \frac{V}{X'_m} E'_m \cos \delta_m \right) \quad (11b)$$

Here, P_L and Q_L are the real and reactive power absorbed by the ZIP-IM model, respectively. The interested reader is referred to [8], [14], [25], [27], [39], for further details regarding ZIP-IM model development and notation.

The dynamic parts of the converter-connected generator model is described by (12)-(13):

$$\begin{aligned} \frac{dE'_g}{dt} &= \frac{1}{T'_{dg}} (E_{FD} - E'_g - (X_g - X'_g) I_d) \\ &= \frac{1}{T'_{dg}} \left(E_{FD} - E'_g \left(\frac{X_g}{X'_g} \right) + \left(\frac{X_g - X'_g}{X'_g} \right) V \cos \delta_g \right) \end{aligned} \quad (12a)$$

$$\begin{aligned} \frac{d\omega_g}{dt} &= \frac{1}{H_g} (T_m - T_e - D\omega_g) \\ &= \frac{1}{H_g} \left(T_m - \frac{VE'_g}{X'_g} \sin \delta_g - D\omega_g \right) \end{aligned} \quad (12b)$$

$$\frac{d\delta_g}{dt} = \omega_g \quad (12c)$$

$$\frac{dV_{DC}}{dt} = \frac{1}{CV_{DC}} (V_{dg} I_{dg} + V_{qg} I_{qg} - V_{DG} I_{DG} - V_{QG} I_{QG}) \quad (12d)$$

$$P_G = \frac{V}{X'_g} E'_g \sin \delta_g + V_{DC} I_{DC} \quad (13a)$$

$$Q_G = \left(\frac{V}{X'_g} E'_g \cos \delta_g - \frac{V^2}{X'_g} \right) + K_q V_{DC} I_{DC} \quad (13b)$$

where P_G and Q_G is the active and reactive power delivered by the converter-connected generator, respectively. Based on (10)–(13), the ADN-model can be represented by a nonlinear seventh-order state-space model; the system states, inputs and outputs are defined as follows: $x = [E'_m, \delta_m, \omega_m, E'_g, \omega_g, \delta, V_{DC}]^T$, $u = [V, \omega_s]^T$ and $y = [P = P_G - P_L, Q = Q_G - Q_L]^T$. The reduced-order system representation of the ADN-model, i.e., the “modified ADN model”, can be obtained by applying a standard state-space decomposition procedure [27]. Further details for the ADN-oriented models can be found in [6]–[8], [27].

REFERENCES

- [1] A. Adrees and J. Milanović, “Effect of load models on angular and frequency stability of low inertia power networks,” *IET Gen. Transm. Distr.*, vol. 13, no. 9, pp. 1520–1526, 2019.
- [2] S. Eftekharijad, V. Vittal, G. T. Heydt, B. Keel, and J. Loehr, “Impact of increased penetration of photovoltaic generation on power systems,” *IEEE Trans. Power Syst.*, vol. 28, no. 2, pp. 893–901, 2013.
- [3] J. V. Milanović, K. Yamashita, S. Martínez Villanueva, S. Z. Djokic, and L. M. Korunović, “International industry practice on power system load modeling,” *IEEE Trans. Power Syst.*, vol. 28, no. 3, pp. 3038–3046, 2013.
- [4] CIGRE, “Modelling of inverter-based generation for power system dynamic studies,” *CIGRE Task Force C4.C6.35*, 2018.

- [5] N. Hatzigiorgiouri, T. Van Cutsem, J. Milanović, P. Pourbeik, C. Vournas, O. Vlachokyriakou, P. Kotsampopoulos, M. Hong, R. Ramos, J. Boemer, P. Aristidou, V. Singhvi, J. Santos, and L. Colombari, “Contribution to bulk system control and stability by distributed energy resources connected at distribution network,” Jan. 2017.
- [6] S. Mat Zali and J. V. Milanović, “Generic model of active distribution network for large power system stability studies,” *IEEE Trans. Power Syst.*, vol. 28, no. 3, pp. 3126–3133, 2013.
- [7] J. V. Milanović and S. Mat Zali, “Validation of equivalent dynamic model of active distribution network cell,” *IEEE Trans. Power Syst.*, vol. 28, no. 3, pp. 2101–2110, 2013.
- [8] *Modelling and Aggregation of Loads in Flexible Power Networks*. Cigre Working Group C4.605, Technical Report, 2014.
- [9] A. Arif, Z. Wang, J. Wang, B. Mather, H. Bashualdo, and D. Zhao, “Load modeling—a review,” *IEEE Trans. Smart Grid*, vol. 9, no. 6, pp. 5986–5999, 2018.
- [10] J. Kim, K. An, J. Ma, J. Shin, K. Song, J. Park, J. Park, and K. Hur, “Fast and reliable estimation of composite load model parameters using analytical similarity of parameter sensitivity,” *IEEE Trans. Power Syst.*, vol. 31, no. 1, pp. 663–671, 2016.
- [11] N. Fulgencio, C. Moreira, L. Carvalho, and J. P. Lopes, “Aggregated dynamic model of active distribution networks for large voltage disturbances,” *Elect. Power Syst. Res.*, vol. 178, 2020.
- [12] The New Aggregated DER Model for Transmission Planning Studies: 2019 Update. EPRI, Palo Alto. 2019. 3002015320.
- [13] G. Chaspierre, G. Denis, P. Panciatici, and T. Van Cutsem, “An active distribution network equivalent derived from large-disturbance simulations with uncertainty,” *IEEE Trans. Smart Grid*, vol. 11, no. 6, pp. 4749–4759, 2020.
- [14] H. Renmu, Ma Jin, and D. J. Hill, “Composite load modeling via measurement approach,” *IEEE Trans. Power Syst.*, vol. 21, no. 2, pp. 663–672, 2006.
- [15] E. O. Kontis, T. A. Papadopoulos, M. H. Syed, E. Guillo-Sansano, G. M. Burt, and G. K. Papagiannis, “Artificial-intelligence method for the derivation of generic aggregated dynamic equivalent models,” *IEEE Trans. Power Syst.*, vol. 34, no. 4, pp. 2947–2956, 2019.
- [16] “Load representation for dynamic performance analysis (of power systems),” *IEEE Trans. Power Syst.*, vol. 8, no. 2, pp. 472–482, 1993.
- [17] W. W. Price, K. A. Wirgau, A. Murdoch, J. V. Mitsche, E. Vaahedi, and M. El-Kady, “Load modeling for power flow and transient stability computer studies,” *IEEE Trans. Power Syst.*, vol. 3, no. 1, pp. 180–187, 1988.
- [18] Y. Li, H. D. Chiang, B. K. Choi, Y. T. Chen, D. H. Huang, and M. G. Lauby, “Representative static load models for transient stability analysis: development and examination,” *IET Gen. Transm. Distr.*, vol. 1, no. 3, pp. 422–431, 2007.
- [19] “Standard load models for power flow and dynamic performance simulation,” *IEEE Trans. Power Syst.*, vol. 10, no. 3, pp. 1302–1313, 1995.
- [20] D. Karlsson and D. J. Hill, “Modelling and identification of nonlinear dynamic loads in power systems,” *IEEE Trans. Power Syst.*, vol. 9, no. 1, pp. 157–166, 1994.
- [21] E. O. Kontis, T. A. Papadopoulos, A. I. Chrysochos, and G. K. Papagiannis, “On the applicability of exponential recovery models for the simulation of active distribution networks,” *IEEE Trans. Power Del.*, vol. 33, no. 6, pp. 3220–3222, 2018.
- [22] G. Mitrentsis and H. Lens, “A dynamic active distribution network equivalent for enhancing the generalization capability of the exponential recovery model in stability studies,” *IEEE Trans. Power Syst.*, vol. 36, no. 3, pp. 2709–2712, 2021.
- [23] W. Xu and Y. Mansour, “Voltage stability analysis using generic dynamic load models,” *IEEE Trans. Power Syst.*, vol. 9, no. 1, pp. 479–493, 1994.
- [24] E. O. Kontis, T. A. Papadopoulos, A. I. Chrysochos, and G. K. Papagiannis, “Measurement-based dynamic load modeling using the vector fitting technique,” *IEEE Trans. Power Syst.*, vol. 33, no. 1, pp. 338–351, 2018.
- [25] Measurement-Based Load Modeling. EPRI, Palo Alto. CA: 2006. 1014402.
- [26] Y. Zhu and J. V. Milanović, “Automatic identification of power system load models based on field measurements,” *IEEE Trans. Power Syst.*, vol. 33, no. 3, pp. 3162–3171, 2018.
- [27] F. Conte, F. D’Agostino, S. Massucco, G. Palombo, F. Silvestro, C. Bossi, and M. Cabiati, “Dynamic equivalent modelling of active distribution networks for TSO-DSO interactions,” in *2017 IEEE PES Innovative Smart Grid Technologies Conference Europe*, 2017, pp. 1–6.
- [28] G. A. Barzegkar-Ntovom, T. A. Papadopoulos, and E. O. Kontis, “Robust framework for online parameter estimation of dynamic equivalent

- models using measurements,” *IEEE Trans. Power Syst.*, vol. 36, no. 3, pp. 2380–2389, 2021.
- [29] DIgSILENT GmbH, DIgSILENT Solutions PowerFactory Version 20.
- [30] Byoung-Kon Choi, Hsiao-Dong Chiang, Yinhong Li, Hua Li, Yung-Tien Chen, Der-Hua Huang, and M. G. Lauby, “Measurement-based dynamic load models: derivation, comparison, and validation,” *IEEE Trans. Power Syst.*, vol. 21, no. 3, pp. 1276–1283, 2006.
- [31] Y. Xu and R. Goodacre, “On splitting training and validation set: A comparative study of cross-validation, bootstrap and systematic sampling for estimating the generalization performance of supervised learning,” *J. Anal. Test.*, vol. 2, no. 3, p. 249–262, 2018.
- [32] A. Saltelli, K. Chan, and E. Scott, *Sensitivity Analysis*. Wiley Series in Probability and Statistics. New York: John Wiley and Sons, 2000.
- [33] J. Ma, D. Han, R. He, Z. Dong, and D. J. Hill, “Reducing identified parameters of measurement-based composite load model,” *IEEE Trans. Power Syst.*, vol. 23, no. 1, pp. 76–83, 2008.
- [34] G. Chaspierre, G. Denis, P. Panciatici, and T. Van Cutsem, “A dynamic equivalent of active distribution network: Derivation, update, validation and use cases,” *IEEE Open Access J. Power Energy*, vol. 8, pp. 497–509, 2021.
- [35] CIGRE, “Benchmark systems for network integration of renewable and distributed energy resources,” *CIGRE Task Force C6.04.02*, 2014.
- [36] IEC Wind Energy Generation Systems – Part 27-1: Electrical Simulations Models – Generic Models, 2020.
- [37] K. N. Hasan, R. Preece, and J. V. Milanović, “The influence of load on risk-based small-disturbance security profile of a power system,” *IEEE Trans. Power Syst.*, vol. 33, no. 1, pp. 557–566, 2018.
- [38] J. L. Hintze and R. D. Nelson, “Violin Plots: A Box Plot-Density Trace Synergism,” *The American Statistician*, vol. 52, no. 2, pp. 181–184, 1998.
- [39] S. Son, S. H. Lee, D. Choi, K. Song, J. Park, Y. Kwon, K. Hur, and J. Park, “Improvement of composite load modeling based on parameter sensitivity and dependency analyses,” *IEEE Trans. Power Syst.*, vol. 29, no. 1, pp. 242–250, 2014.